HHS Public Access

Author manuscript

Epilepsy Res. Author manuscript; available in PMC 2017 February 01.

Published in final edited form as:

Epilepsy Res. 2016 February ; 120: 47–54. doi:10.1016/j.eplepsyres.2015.11.005.

Widespread Neuronal Injury In A Model Of Cholinergic Status Epilepticus In Postnatal Day 7 Rat Pups

Daniel Torolira[1,*], **Lucie Suchomelova**[1,*], **Claude G. Wasterlain**[1,2,3], and **Jerome Niquet**[1,2,#]

[1]Epilepsy Research Laboratory (151), Veterans Affairs Greater Los Angeles Healthcare System, Los Angeles, CA

[2]Department of Neurology, David Geffen School of Medicine at UCLA, Los Angeles, CA

[3]Brain Research Institute, David Geffen School of Medicine at UCLA, Los Angeles, CA

Introduction

Status Epilepticus (SE) is common in neonates and infants. In the neonatal period seizures are the most common neurological symptom with an incidence of approximately 1.8–3.5 per 1000 live births, which represents the greatest incidence of seizures throughout the human life span (Cowan, 2002; Silverstein and Jensen, 2007; Wirrell, 2005). Neonatal seizures are often associated with adverse developmental outcomes and increased prevalence of epilepsy (Volpe, 2001; Zupanc, 2004).

Previous animal models of SE in the immature brain have proven very useful in examining the long-term consequences of SE and evaluating possible therapeutic avenues. In the lithium pilocarpine model, for instance, SE results in neuronal injury as early as postnatal day 12–14 (P12) (Druga et al., 2010; Ekstrand et al., 2011; Kubova et al., 2002; Kubova et al., 2001; Sankar et al., 2000; Sankar et al., 1998; Suchomelova et al., 2006). However, other studies and models have been unable to find significant SE-induced neuronal injury at ages earlier than P12, unless seizures are combined with inflammatory stressors such as lipopolysaccharide (Auvin et al., 2007). It is not clear whether this is due to an inherent resistance of the neonatal brain to SE-induced neuronal injury, or to our limited ability to treat SE and reduce its mortality in rodent models.

[#]Corresponding author: Epilepsy Research Laboratory, VA Greater Los Angeles Healthcare System., 11301 Wilshire Boulevard. Building 114, Room 139. West Los Angeles, CA 90073. Phone number: (310) 478-3711 ext. 41974, Fax number: (310) 268 4856, jniquet@ucla.edu.

[*]Lucie Suchomelova and Daniel Torolira contributed equally to this study.

We confirm that we have read the Journal's position on issues involved in ethical publication and affirm that this report is consistent with those guidelines.

Disclosure of Conflicts of Interest

No authors have any conflict of interest to disclose.

A model of severe neonatal SE with high survival would give us insight into long-term consequences of SE in the neonatal brain, its potential for recovery, and the beneficial or adverse effects of various treatments. In the present study, we have developed a model of cholinergic SE in P7 rats, which combines high survival rates and widespread irreversible neuronal injury. It provides a valuable tool to study the relationship between seizures, GABAergic drugs and neuronal injury, as well as the neonatal brain's long-term response to SE- or treatment-associated brain damage.

Materials and methods

2.1. Animals

Male and female Sprague-Dawley albino rats (Charles River Laboratories, San Diego, CA) 7 days old (P7, n=48), were used. The day of birth was considered as day 0. All animals were housed in a temperature- and humidity- controlled room with 12h light-dark cycles (light cycle starts at 7 am) and had free access to food and water. All experiments were conducted with the approval of and in accordance with the regulations of the Institutional Animal Care and Use Committee of West Los Angeles VA Medical Center.

Induction of SE

This model was designed to mimic the seizures induced by 1.6/2 × LD50 of soman in adult rats (Tetz et al., 2006) and was adapted by us for use in P7 pups. Lithium chloride (LiCl, 5 mEq/kg) was administered intraperitoneally (i.p.) at P6 and the next day, SE was induced with subcutaneous pilocarpine hydrochloride (Pilo, 320 mg/kg, i.p.) together with scopolamine methyl chloride (1mg/kg, i.p.) to block peripheral effect of pilocarpine. Pups were kept in the special warming chamber to maintain their normal temperature (34–35°C). Behavioral seizures are rated on a 1–3 scale where 1 is motor hyperactivity, 2 is clonic activity, and 3 is running seizures with vocalization. All animals were rehydrated with saline approximately 4 h after SE (10% of body weight, s.c.). Rats were sacrificed either 6 h (SE6HRS, n=10) or 24 h (SE24HRS, n=26) after SE onset. Control groups included rats naïve to treatment (Sham, n=5), rats injected with only LiCl (LiCl, n=7) or only Pilo (Pilo, n=4).

2.3. Acute EEG recording and physiology

In order to characterize the status epilepticus in P7 pups, additional animals were prepared for EEG recording. Under isoflurane anesthesia (2–5%), tripolar registration electrodes (Plastic One, Roanoke, VA) were implanted over the right and left occipital cortex (coordinates AP=3.5mm, L=3 mm) one day before SE (P6). The ground middle electrode wire was implanted over the frontal cortex. Electrodes were anchored with adhesive and dental cement. After surgery, pups were kept on a 35°C heating pad until returned to their dams. Lithium was administered on the day of surgery. One day later (P7), EEG electrodes were connected to tethered cables with swivel mounts (Plastic One, Roanoke, VA), which fed the signal to a monitoring and recording system (AcqKnowledge, Biopac System). After 5 h of continuous recording, the animals were returned to their mother. EEG recording started 15 min prior to pilocarpine administration (baseline). The severity of SE was assessed as previously described (Suchomelova et al., 2006) with modifications by

measuring the following parameters: latency to onset of SE (timed from pilocarpine injection to onset of first behavioral seizure), continuous polyspike activity (timed from onset of first seizure until continuous seizure activity was interrupted for at least 1 min), number of seizures, mean seizure duration, duration of SE (time from the onset of SE to the end of the last seizure, including interictal time), and total seizure time (total time spent in seizures, timed from the onset of SE, subtracting interictal time).

O_2 saturation was measured non-invasively from paw probes using PhysioSuite monitor (Kent Scientific, CT) in selected animals beginning 10 minutes before pilocarpine and continuing for 90 minutes after pilocarpine administration.

2.4. Preparation of tissue for immunohistochemistry and detection of neuronal injury

Rats were then perfused at either 6 h after SE induction (SE6Hrs) or 24 h (SE24Hrs). Control groups (Sham, LiCL, and Pilo) were sacrificed at the same age as the SE24Hrs group (P8). Pups were anesthetized with an overdose of pentobarbital and then underwent transcardiac perfusion with 2% phosphate-buffered paraformaldehyde. Brains were kept in situ at 4 °C overnight and then removed and postfixed in the same perfusate for 2 h. Subsequently, brains were dehydrated, embedded in paraffin and cut into 10 μm-thick coronal sections. Brain sections were then deparaffinized before being subjected to caspase-3a immunohistochemistry or fluoro-Jade B (FJB) staining procedure. For FJB detection, sections were incubated with 0.06% KMnO4 followed by 0.001% FJB and evaluated under fluorescent light (Schmued et al., 1997).

For identification of neuronal injury in the hippocampus (CA1/subiculum, DG, and CA3), three adjacent sections in dorsal hippocampus (approximately 3.30 mm posterior to Bregma) and three adjacent sections in ventral hippocampus (approximately 5.30 mm posterior to Bregma) were used for a total of six sections per animal. Manual counting of FJB-positive (FJB+) cells was performed with a Leica 40× objective along the whole length of CA1/subiculum, CA3, and the dentate gyrus granule cell layer (DG) of both the left and right sides of the hippocampus. To compensate for anatomical variations, the length of CA1/subiculum, CA3, and DG in each field was measured and the average number of positive cells was expressed per mm length of each specific hippocampal structure. After computing an average value (FJB+ cells/mm) of left and right CA1/subiculum, DG, and CA3 (for both dorsal and ventral hippocampus), the two sides were averaged for a final FJB+ cell ratio of dorsal and ventral hippocampus.

For identification of neuronal injury in the thalamus and neocortex, two adjacent sections including dorsal hippocampus (~Bregma −3.30 mm) were manually counted with a Leica 10× objective, averaged per animal, and then subjected to a 6-point scoring system based on the data variability and range. For this system, a score of “0” indicated 0 positive cells in the field, “1” indicated 1–15 cells, “2” indicated 16–30 cells, “3” indicated 31–50 cells, “4” indicated 51–100 cells, “5” indicated 101–200 cells, and “6” indicated 200-plus cells. Because no discernable pattern of damage between thalamic nuclei was found, all FJB+ cells in the thalamus were counted as a whole. Parietal cortex was defined as the cortical area from the curved tip of the cingulum down to the rhinal fissure. Neocortical counting

was not layer-specific, however notes of any injury patterns were made for each animal and reported in the results.

Additionally, the following brain structures were also observed: caudate putamen, nucleus accumbens, septal nuclei, piriform cortex, globus pallidus, ventral pallidum, amygdala, hypothalamus, substantia nigra, and lateral entorhinal cortex. For analysis of neuronal injury in other brain regions, a random subset of SE24HRS and Sham pups were chosen at random. From each animal, two adjacent sections per brain region were manually counted using a Leica 10× objective and then averaged per animal. For instance, two rostral sections (~Bregma 1.2 mm) including caudate putamen and two caudal sections (~Bregma −6.0 mm) including lateral entorhinal cortex were analyzed per animal. To compensate for anatomical variations between sections, the area of each structure per field was measured and the average number of FJB+ cells was expressed per mm^2 of each brain area.

2.5. Immunohistochemical studies for active caspase-3 (caspase-3a)

Detection of caspase-3a-immunoreactive (IR) cells was performed as described previously (Lopez-Meraz et al., 2010). Manual counting of caspase-3a-IR cells was performed bilaterally in the CA1-subiculum, thalamus, and neocortex using a Leica 40× objective. Three adjacent sections including dorsal hippocampus (~Bregma −3.30 mm) were taken from a randomly chosen subset of SE24HRS (n=5) and compared to Sham controls (n=5). The total number of caspase-3a IR cells were averaged per animal and reported. After caspase-3 IR cell counts were completed, images were captured and coverslips removed for identification of neuronal damage. FJB staining was performed as above and the percentage of FJB+ cells expressing caspase-3a was calculated in three sections (~Bregma −3.30 mm) per animal.

2.6. Statistical Analysis

Experimental groups that showed different variances were analyzed with non parametric statistical methods: Kruskal–Wallis one-way ANOVA followed by Dunn's test, Mann–Whitney, or Holm Sidak test versus the control groups. Statistical significances were considered when $p<0.05$. In all graphs, data are presented as the mean ± S.E.M.

Results

3.1. The course of SE in P7 pups

The combination of high-dose lithium (5 mEq/kg) and pilocarpine (320 mg/kg, i.p.) induced SE in 103 out of 138 pups (74.6%). Immediately after pilocarpine injection, pups became hyperactive. The first epileptiform spikes appeared after 6.2±1.8 min., and the first EEG seizure appeared after 8.2±1.8 min. (Fig 1A). Behavioral seizure manifestations varied from forelimbs clonus (stage 2) to running seizures with vocalization (stage 3). Only the animals that reached stage 3 were included in the study. Nearly continuous polyspike activity which lasted approximately 50 min was interrupted by progressively increasing periods of interictal low-voltage activity and evolved into periodic epileptiform discharges. We measured the number, the mean duration and total duration of these discharges (Fig 1B). The survival rate

was 72/103 (69.9%) by 24 h post-SE onset. The animals did not show significant hypoxemia during SE (Fig. 1C).

Distribution of neuronal injury after SE

CA1—Neuronal injury in the stratum pyramidale of dorsal and ventral CA1/subiculum was examined in Sham, LiCl, and Pilocarpine controls and at 6 and 24 h after SE induction (Fig. 2). Very little neuronal FJB staining was found among Sham, LiCl, and Pilo pups. At 6 h post-SE, very few degenerating neurons were evident in CA1/subiculum. However, by 24 h post-SE significant neuronal injury of pyramidal cells in CA1/subiculum was evident in both dorsal and ventral hippocampus. The distribution of FJB-stained cells was predominantly in subiculum and in the adjacent segment of CA1 in SE24HRS pups (Supplemental Fig. 1). Among CA1 pyramidal cells, the FJB cell distribution was mainly found in the upper layer although a small number (<5 cells per field) of FJB+ cells were occasionally found in the stratum oriens (data not shown).

CA3—Few FJB+ neurons were found in CA3 of Sham, LiCl, and Pilo pups. However, at 6 h post-SE we observed significant cell injury in the stratum pyramidale of dorsal but not of ventral CA3. This injury was significantly different from all control groups (Fig. 3B). However, neuronal injury in the SE6Hrs pups was not limited to the pyramidal cell layer. As seen in Fig. 3A, some degenerating neurons were also found in the stratum oriens and stratum lucidum. Six h after SE onset, in 3/10 pups the stratum oriens and lucidum combined contained >5 FBJ-stained cells per field, while in the remaining 7 these layers showed <5 FBJ-stained cells per field. At 24 h post-SE, the number of FJB-stained neurons of dorsal CA3 showed a non-significant downward trend compared to SE6Hrs while a few injured neurons appeared in ventral CA3 (Fig. 3C).

DG—Very few FJB+ cells were found in dorsal and ventral DG among Sham, LiCl, and Pilo pups. At 6 h, neuronal injury was significantly different from controls in dorsal but not ventral DG (Fig. 2D). By 24 h post-SE, however, neuronal injury in both dorsal and ventral DG was significantly greater than in SE6Hrs pups and controls. Interestingly, there was no significant increase in FJB+ cells in the hilus in any group. Additionally, as shown in Supplemental Figure 2A, FJB+ cell density in DG granule cell layer varied dramatically between animals.

Neocortex—Neocortex was examined for neuronal injury in sections that included dorsal hippocampus (~Bregma −3.30 mm) (Fig. 4). In both SE6Hrs and SE24Hrs pups, parietal cortex showed significantly more degenerating neurons than in Sham, LiCl, and Pilo controls. As shown in Figure 4A, neuronal injury in parietal cortex was consistenly found along layer 2, although some FJB+ cells were spread throughout layer 4 and other cortical layers as well.

Thalamus—Thalamic nuclei in sections including dorsal hippocampus (~Bregma −3.30 mm) showed significant neuronal injury compared to controls at 6 h and this increased by 24 h (Fig. 4D). Figure 4C shows neuronal injury that predominates in dorsolateral nuclei, but in other rats injury was abundant in ventromedial or other nuclei.

Other Limbic regions—We found significant FJB staining in the amygdala and piriform cortex in SE24Hrs pups compared to Sham (Fig. 5). As in the thalamus, injury among amygdaloid nuclei varied and, therefore, the structure was counted as a whole. In addition, lateral entorhinal cortex and hypothalamus also showed significantly increased neuronal injury in SE24Hrs pups when compared to Sham. The septal nuclei, however, showed no significant increase in neuronal injury due to SE, even at the 24 h post-SE time point.

Basal ganglia—In caudate/putamen of SE24Hrs pups we found a striking increase in FJB-staining when compared to controls (Fig. 5). Likewise, nucleus accumbens (including its shell) showed a significant increase in neuronal injury. Finally, globus pallidus and ventral pallidum displayed significant cell injury in SE24Hrs animals when compared to Sham. The substantia nigra and superior colliculus had no FJB-staining (data not shown).

As shown in Table 1, this neuronal injury can vary among brain regions between different animals, reflecting the inherent variability of the lithium-pilocarpine model. While some animals had most neuronal injury concentrated in hippocampus, others showed damage most prominently in neocortex or thalamus and vice versa. As evident from Table 1, comparison of cell injury between dorsal CA1 and thalamus reveals that 3 animals had cell damage above the median in both areas, 20 animals had cell damage above the median in one of the two areas, and only 3/26 animals had cell damage below the median in both areas. The 3 animals (#11, 17, 25) with cell damage below the median in dorsal CA1 and thalamus, however, all had cell damage above the median in parietal cortex. Importantly, there are no animals that have cell damage below the median in all areas.

SE triggers an active form of cell death in CA1, thalamus, and neocortex The contribution of caspase-3 to SE-induced neuronal death was assessed by light immunohistochemistry using an antibody which recognizes caspase-3a, the active form of that enzyme. At 24 h post-SE, caspase-3a immunoreactivity (IR) was significantly increased in CA1/subiculum, thalamus, and neocortex compared to Sham (Fig. 6). Cell counting showed that the percentage of FJB-positive cells expressing caspase-3a in the thalamus, neocortex and CA1/subiculum was respectively 75 ± 17%, 56 ± 12% and 34 ± 9%. As shown in Fig. 6, these caspase-3a IR cells have distinct changes in nuclear morphology, such as fragmented nuclei, suggesting that SE triggers an irreversible form of cell injury. A few caspase-3a positive cells were also found in CA3 and DG (data not shown).

Discussion

We have developed a model of neonatal SE at P7 with relatively high survival (70%) that for the first time induces widespread irreversible neuronal injury throughout the brain. Oxygen saturation data show that this neuronal injury is not the result of hypoxemia. Many studies have reported a lack of lesions after SE before P12, unless seizures are combined with inflammatory stressors (Auvin et al., 2007). For instance, seizures induced in immature rats (<P12) by kainate (Ben-Ari et al., 1984; Lopez-Picon et al., 2004; Rizzi et al., 2003), pilocarpine (Cavalheiro et al., 1987), flurothyl (Wasterlain, 1976) or lithiumpilocarpine (Dube et al., 1998) reportedly show little or no neuronal loss. These findings have fostered the concept of an intrinsic resistance of the immature brain to neuronal injury. However,

given our results, we may need to reconsider to what extent this resistance may reflect the high mortality associated with animal models of neonatal seizures. Newborn humans are treated in neonatal intensive care units (ICUs), many survive with brain damage, and SE is an independent risk factor for poor outcome (Pisani et al., 2007). If ICU treatment were available for rodent pups, survival rates might be higher, and some survivors might show brain damage. The severity and long duration (271±10 min) of SE in this model might also play a role. Kainic acid SE in immature rats is mild, because the dose used to induce SE in adults cannot be used in neonates where it is uniformly fatal. The dose of kainate used to induce SE in neonates also fails to cause neuronal injury in adults. An alternative explanation is that injury may be model-specific, perhaps related to the cholinergic nature of SE in the current model and it is uncertain whether it applies to other types of severe neonatal seizures (Holmes et al., 1998; Liu et al., 1999; Riviello et al., 2002). This would have implications for neonatal victims of SE induced by nerve agents or organophosphates, although the lack of lesions when neonatal SE is induced by nerve agents in experimental animals argues against that interpretation (Miller et al., 2015). At 6 h post-SE onset, we found mild but significant neuronal injury in neocortex, thalamus, CA3 and dentate gyrus of the dorsal hippocampal formation. However, by 24 h post-SE we observed more widespread damage in both dorsal and ventral parts of hippocampal formation, neocortex, and thalamus, suggesting that neuronal injury increases progressively after the onset of SE. In addition, by 24 h post-SE we found significant brain damage in basal ganglia structures (caudate putamen, nucleus accumbens, globus pallidus, ventral pallidum) and other limbic regions (amygdala, piriform cortex, lateral entorhinal cortex, hypothalamus), indicating that severe neonatal SE can result in injury throughout the brain. Interestingly, hilar interneurons were preserved in this model. This confirms earlier reports from our laboratory (Sankar et al., 1998) showing that hilar interneurons are less susceptible to seizure in the immature than in the mature brain.

This new model may be useful in examining long-term effects of SE-induced neuronal injury in the neonatal brain. Previous studies have shown that recurring early-life seizures or SE resulted in developmental delays (Wasterlain, 1977), spatial learning impairments and memory deficits (Baram, 2003; Bo et al., 2004; de Rogalski Landrot et al., 2001; Holmes et al., 1998; Huang et al., 1999; Karnam et al., 2009a; Karnam et al., 2009b; Liu et al., 2003; Sayin et al., 2004). In addition, SE in the immature brain has been associated with the development of epileptogenesis (Lynch et al., 2000; Sankar et al., 2000; Suchomelova et al., 2006) and a reduction of hippocampal volume when measured in adulthood (Nairismagi et al., 2006). In this study, neuronal injury involved areas where neurons are post-mitotic, such as CA1/subiculum, as well as areas where neurogenesis is quite active, such as dentate granule cells. It will be interesting to see whether these regions differ in their potential for anatomical and functional recovery.

Furthermore, this model may help clarify whether GABAergic drugs, which are the standard clinical treatment, can further increase seizure-associated neuronal injury in vivo. Experimental evidence indicates that GABAergic drugs can have excitatory effects, aggravate seizures, increase neuronal injury, and make seizures harder to control in the neonatal brain (Ben-Ari, 2014; Dzhala and Staley, 2003; Dzhala et al., 2005; Staley, 1992). In conclusion, this model provides a valuable tool that can be used to evaluate the neonatal

brain's response to SE-induced brain damage and to standard clinical treatments, both acutely and chronically.

Supplementary Material

Refer to Web version on PubMed Central for supplementary material.

Acknowledgments

This work was supported in part by Merit Review Award # I01 BX000273-07 from the United States (U.S.) Department of Veterans Affairs (Biomedical Laboratory Research and Development Service) and NINDS (grant UO1 NS074926; CW).

REFERENCES

Auvin S, Shin D, Mazarati A, Nakagawa J, Miyamoto J, Sankar R. Inflammation exacerbates seizure-induced injury in the immature brain. Epilepsia. 2007; 48(Suppl 5):27–34. [PubMed: 17910578]

Baram TZ. Long-term neuroplasticity and functional consequences of single versus recurrent early-life seizures. Ann Neurol. 2003; 54:701–705. [PubMed: 14681879]

Ben-Ari Y. The GABA excitatory/inhibitory developmental sequence: a personal journey. Neuroscience. 2014; 279:187–219. [PubMed: 25168736]

Ben-Ari Y, Tremblay E, Berger M, Nitecka L. Kainic acid seizure syndrome and binding sites in developing rats. Brain Res. 1984; 316:284–288. [PubMed: 6467019]

Bo T, Jiang Y, Cao H, Wang J, Wu X. Long-term effects of seizures in neonatal rats on spatial learning ability and N-methyl-D-aspartate receptor expression in the brain. Brain Res Dev Brain Res. 2004; 152:137–142. [PubMed: 15351501]

Cavalheiro EA, Silva DF, Turski WA, Calderazzo-Filho LS, Bortolotto ZA, Turski L. The susceptibility of rats to pilocarpine-induced seizures is agedependent. Brain Res. 1987; 465:43–58. [PubMed: 3440212]

Cowan LD. The epidemiology of the epilepsies in children. Ment Retard Dev Disabil Res Rev. 2002; 8:171–181. [PubMed: 12216061]

de Rogalski Landrot I, Minokoshi M, Silveira DC, Cha BH, Holmes GL. Recurrent neonatal seizures: relationship of pathology to the electroencephalogram and cognition. Brain Res Dev Brain Res. 2001; 129:27–38. [PubMed: 11454410]

Druga R, Mares P, Kubova H. Time course of neuronal damage in the hippocampus following lithium-pilocarpine status epilepticus in 12-day-old rats. Brain Res. 2010; 1355:174–179. [PubMed: 20673826]

Dube C, Andre V, Covolan L, Ferrandon A, Marescaux C, Nehlig A. C-Fos, Jun D and HSP72 immunoreactivity, and neuronal injury following lithium-pilocarpine induced status epilepticus in immature and adult rats. Brain Res Mol Brain Res. 1998; 63:139–154. [PubMed: 9838083]

Dzhala VI, Staley KJ. Excitatory actions of endogenously released GABA contribute to initiation of ictal epileptiform activity in the developing hippocampus. J Neurosci. 2003; 23:1840–1846. [PubMed: 12629188]

Dzhala VI, Talos DM, Sdrulla DA, Brumback AC, Mathews GC, Benke TA, Delpire E, Jensen FE, Staley KJ. NKCC1 transporter facilitates seizures in the developing brain. Nat Med. 2005; 11:1205–1213. [PubMed: 16227993]

Ekstrand JJ, Pouliot W, Scheerlinck P, Dudek FE. Lithium pilocarpine-induced status epilepticus in postnatal day 20 rats results in greater neuronal injury in ventral versus dorsal hippocampus. Neuroscience. 2011; 192:699–707. [PubMed: 21669257]

Holmes GL, Gairsa JL, Chevassus-Au-Louis N, Ben-Ari Y. Consequences of neonatal seizures in the rat: morphological and behavioral effects. Ann Neurol. 1998; 44:845–857. [PubMed: 9851428]

Huang L, Cilio MR, Silveira DC, McCabe BK, Sogawa Y, Stafstrom CE, Holmes GL. Long-term effects of neonatal seizures: a behavioral, electrophysiological, and histological study. Brain Res Dev Brain Res. 1999; 118:99–107. [PubMed: 10611508]

Karnam HB, Zhao Q, Shatskikh T, Holmes GL. Effect of age on cognitive sequelae following early life seizures in rats. Epilepsy Res. 2009a; 85:221–230. [PubMed: 19395239]

Karnam HB, Zhou JL, Huang LT, Zhao Q, Shatskikh T, Holmes GL. Early life seizures cause long-standing impairment of the hippocampal map. Exp Neurol. 2009b; 217:378–387. [PubMed: 19345685]

Kubova H, Druga R, Haugvicova R, Suchomelova L, Pitkanen A. Dynamic changes of status epilepticus-induced neuronal degeneration in the mediodorsal nucleus of the thalamus during postnatal development of the rat. Epilepsia. 2002; 43(Suppl 5):54–60. [PubMed: 12121296]

Kubova H, Druga R, Lukasiuk K, Suchomelova L, Haugvicova R, Jirmanova I, Pitkanen A. Status epilepticus causes necrotic damage in the mediodorsal nucleus of the thalamus in immature rats. J Neurosci. 2001; 21:3593–3599. [PubMed: 11331388]

Liu X, Muller RU, Huang LT, Kubie JL, Rotenberg A, Rivard B, Cilio MR, Holmes GL. Seizure-induced changes in place cell physiology: relationship to spatial memory. J Neurosci. 2003; 23:11505–11515. [PubMed: 14684854]

Liu Z, Yang Y, Silveira DC, Sarkisian MR, Tandon P, Huang LT, Stafstrom CE, Holmes GL. Consequences of recurrent seizures during early brain development. Neuroscience. 1999; 92:1443–1454. [PubMed: 10426498]

Lopez-Meraz ML, Wasterlain CG, Rocha LL, Allen S, Niquet J. Vulnerability of postnatal hippocampal neurons to seizures varies regionally with their maturational stage. Neurobiol Dis. 2010; 37:394–402. [PubMed: 19879360]

Lopez-Picon F, Puustinen N, Kukko-Lukjanov TK, Holopainen IE. Resistance of neurofilaments to degradation, and lack of neuronal death and mossy fiber sprouting after kainic acid-induced status epilepticus in the developing rat hippocampus. Neurobiol Dis. 2004; 17:415–426. [PubMed: 15571977]

Lynch M, Sayin U, Bownds J, Janumpalli S, Sutula T. Long-term consequences of early postnatal seizures on hippocampal learning and plasticity. Eur J Neurosci. 2000; 12:2252–2264. [PubMed: 10947804]

Miller SL, Aroniadou-Anderjaska V, Figueiredo TH, Prager EM, Almeida-Suhett CP, Apland JP, Braga MF. A rat model of nerve agent exposure applicable to the pediatric population: The anticonvulsant efficacies of atropine and GluK1 antagonists. Toxicol Appl Pharmacol. 2015; 284:204–216. [PubMed: 25689173]

Nairismagi J, Pitkanen A, Kettunen MI, Kauppinen RA, Kubova H. Status epilepticus in 12-day-old rats leads to temporal lobe neurodegeneration and volume reduction: a histologic and MRI study. Epilepsia. 2006; 47:479–488. [PubMed: 16529609]

Pisani F, Cerminara C, Fusco C, Sisti L. Neonatal status epilepticus vs recurrent neonatal seizures: clinical findings and outcome. Neurology. 2007; 69:2177–2185. [PubMed: 18056582]

Riviello P, de Rogalski Landrot I, Holmes GL. Lack of cell loss following recurrent neonatal seizures. Brain Res Dev Brain Res. 2002; 135:101–104. [PubMed: 11978398]

Rizzi M, Perego C, Aliprandi M, Richichi C, Ravizza T, Colella D, Veliskova J, Moshe SL, De Simoni MG, Vezzani A. Glia activation and cytokine increase in rat hippocampus by kainic acid-induced status epilepticus during postnatal development. Neurobiol Dis. 2003; 14:494–503. [PubMed: 14678765]

Sankar R, Shin D, Mazarati AM, Liu H, Katsumori H, Lezama R, Wasterlain CG. Epileptogenesis after status epilepticus reflects age- and model-dependent plasticity. Ann Neurol. 2000; 48:580–589. [PubMed: 11026441]

Sankar R, Shin DH, Liu H, Mazarati A, Pereira de Vasconcelos A, Wasterlain CG. Patterns of status epilepticus-induced neuronal injury during development and long-term consequences. J Neurosci. 1998; 18:8382–8393. [PubMed: 9763481]

Sayin U, Sutula TP, Stafstrom CE. Seizures in the developing brain cause adverse long-term effects on spatial learning and anxiety. Epilepsia. 2004; 45:1539–1548. [PubMed: 15571512]

Schmued LC, Albertson C, Slikker W Jr. Fluoro-Jade: a novel fluorochrome for the sensitive and reliable histochemical localization of neuronal degeneration. Brain Res. 1997; 751:37–46. [PubMed: 9098566]

Silverstein FS, Jensen FE. Neonatal seizures. Ann Neurol. 2007; 62:112–120. [PubMed: 17683087]

Staley K. Enhancement of the excitatory actions of GABA by barbiturates and benzodiazepines. Neurosci Lett. 1992; 146:105–107. [PubMed: 1282225]

Suchomelova L, Baldwin RA, Kubova H, Thompson KW, Sankar R, Wasterlain CG. Treatment of experimental status epilepticus in immature rats: dissociation between anticonvulsant and antiepileptogenic effects. Pediatr Res. 2006; 59:237–243. [PubMed: 16439585]

Tetz LM, Rezk PE, Ratcliffe RH, Gordon RK, Steele KE, Nambiar MP. Development of a rat pilocarpine model of seizure/status epilepticus that mimics chemical warfare nerve agent exposure. Toxicol Ind Health. 2006; 22:255–266. [PubMed: 16924957]

Volpe, J. Philadelphia, PA: WB Saunders; 2001. Neonatal seizures, Neurology of the newborn.

Wasterlain CG. Effects of neonatal status epilepticus on rat brain development. Neurology. 1976; 26:975–986. [PubMed: 986588]

Wasterlain CG. Effects of neonatal seizures on ontogeny of reflexes and behavior. An experimental study in the rat. Eur Neurol. 1977; 15:9–19. [PubMed: 856589]

Wirrell EC. Neonatal seizures: to treat or not to treat? Semin Pediatr Neurol. 2005; 12:97–105. [PubMed: 16114175]

Zupanc ML. Neonatal seizures. Pediatr Clin North Am. 2004; 51:961–978. ix. [PubMed: 15275983]

Highlights

- Cholinergic status epilepticus was induced with high-dose lithium and pilocarpine in postnatal day 7 rat pups.
- EEGs showed continuous polyspikes activity for 54.3 ± 6.7 min, while O2 saturation showed no significant hypoxemia.
- Widespread neuronal injury (fluoro-jade B staining) and increase in caspase-3a IR were observed by 24 h after SE onset.
- Caspase-3a-IR neurons had fragmented nuclei, suggesting that SE triggered an irreversible form of cell injury.

A.

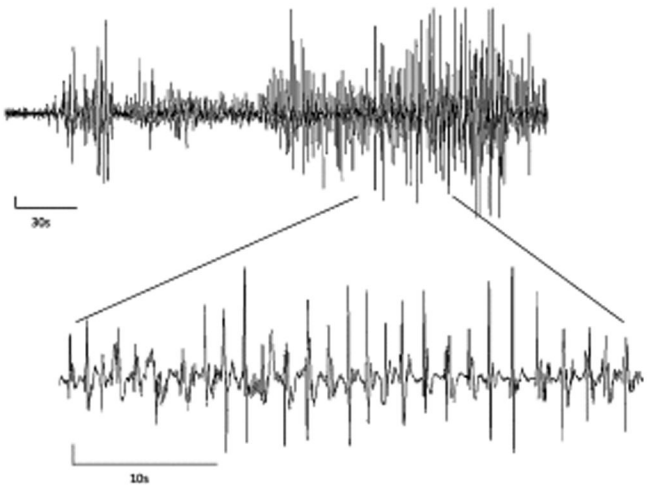

B.

Parameters	Mean± SE	# of animals
Latency to first EEG seizure	8.2±1.8	15
Continuous seizure activity	54.3±6.7	8
Number of seizures	48.5±4.2	8
Mean seizure duration	24.7±3.2	8
Cumulative seizure time	18.9±2.6	8
Total seizure time	73.1±7.3	8
Duration of SE	271±10.3	8

C.

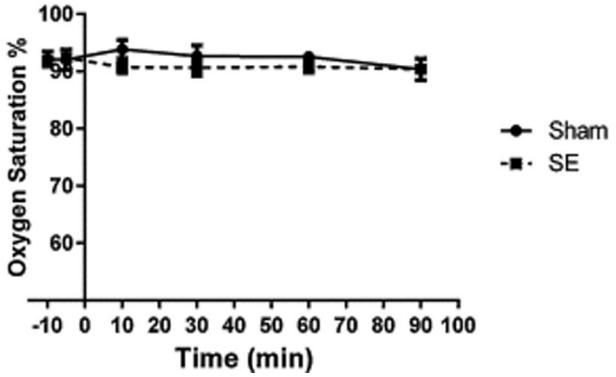

Figure 1.

The course of SE in P7 pups. (A) Representative EEG trace during SE. (B) EEG parameters during SE. (C) Time course of oxygen saturation. There was no significant hypoxemia during SE.

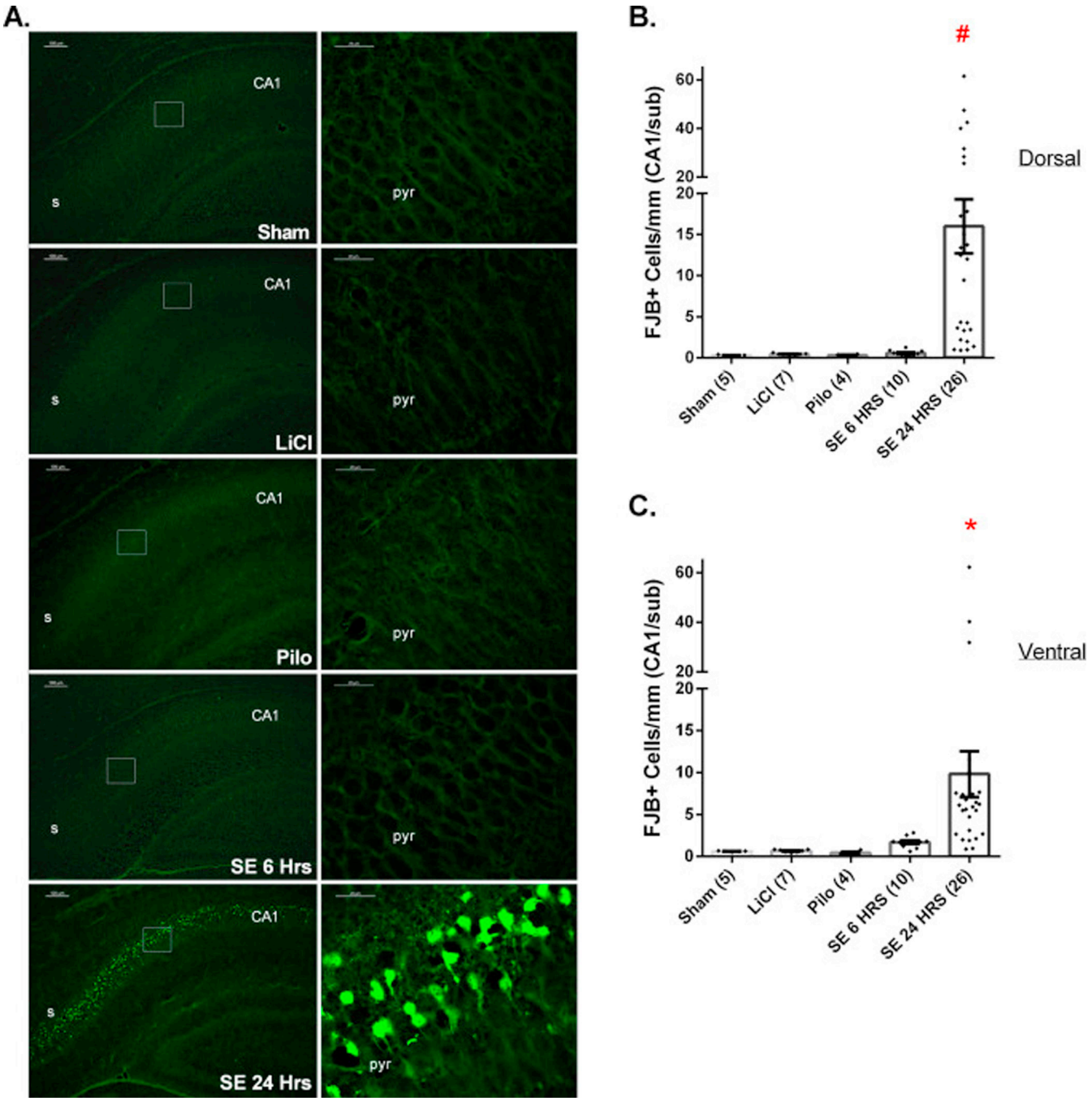

Figure 2.

SE results in significant neuronal injury in both dorsal and ventral CA1/Subiculum and dentate gyrus in P7 rat pups by the 24 h post-SE time period. (A) Images of FJB staining among Sham, LiCl, Pilo, SE6Hrs, and SE24Hrs animals. The image on the right of each row is a higher magnification of the boxed area on the image on the left. (B, C) Extent of neuronal injury in dorsal (B) and ventral (C) CA1/subiculum pyramidal cell layer. (B) #: $p<0.05$: SE24HRS vs. Sham, LiCl, Pilo, SE6HRS (analyzed by Dunn's test). (C) *: $p<0.05$: SE24HRS vs. Sham, LiCl, Pilo (Dunn's test) or vs. SE6HRS (Mann-Whitney test).

Abbreviations: s=Subiculum, CA1=cornus ammonis region 1, pyr=stratum pyrimidale. Scale bars: (A) left column=100 μm (low magnification images) and right column 20 μm (high magnification images).

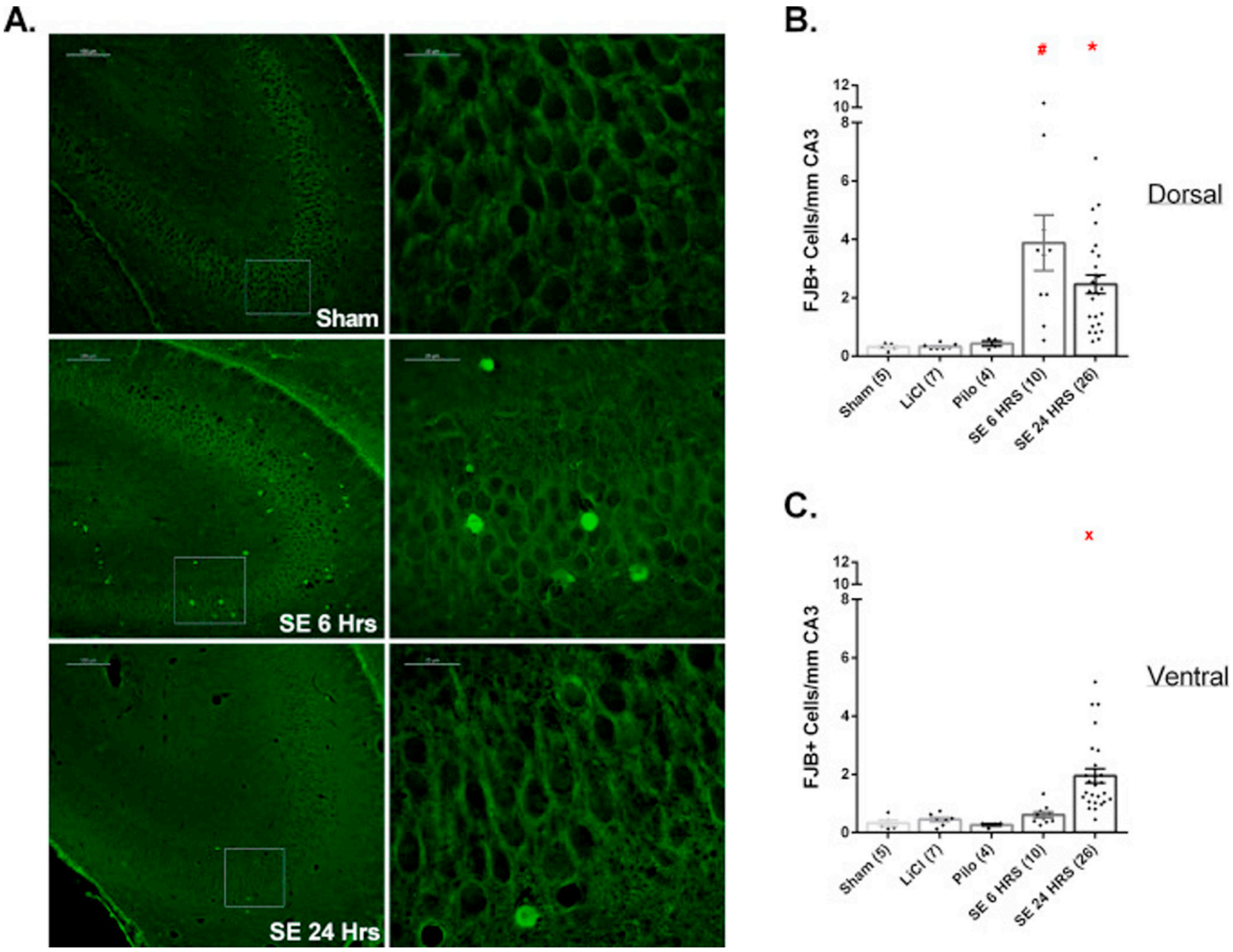

Figure 3.

SE results in significant neuronal injury in dorsal/ventral CA3.

(A). Images of FJB staining in CA3 among Sham, SE6Hrs, and SE24Hrs animals. The image on the right of each row is a higher magnification of the boxed area on the image on the left. (B, C) Extent of neuronal injury in dorsal (B) and ventral (C) CA3 pyramidal cell layer. (B) # $p<0.05$: SE 6 HRS vs. Sham, LiCl, Pilo (analyzed by Dunn's test). * $p<0.05$: SE 24 HRS vs. Sham, LiCl (Dunn's test); vs. Pilo (Mann-Whitney test). (C) × $p<0.05$: SE 24 HRS vs. Sham, LiCl, Pilo, SE 6 HRS (Dunn's test). Scale bars: (A) left column=100 μm (low magnification images) and right column 20 μm (high magnification images).

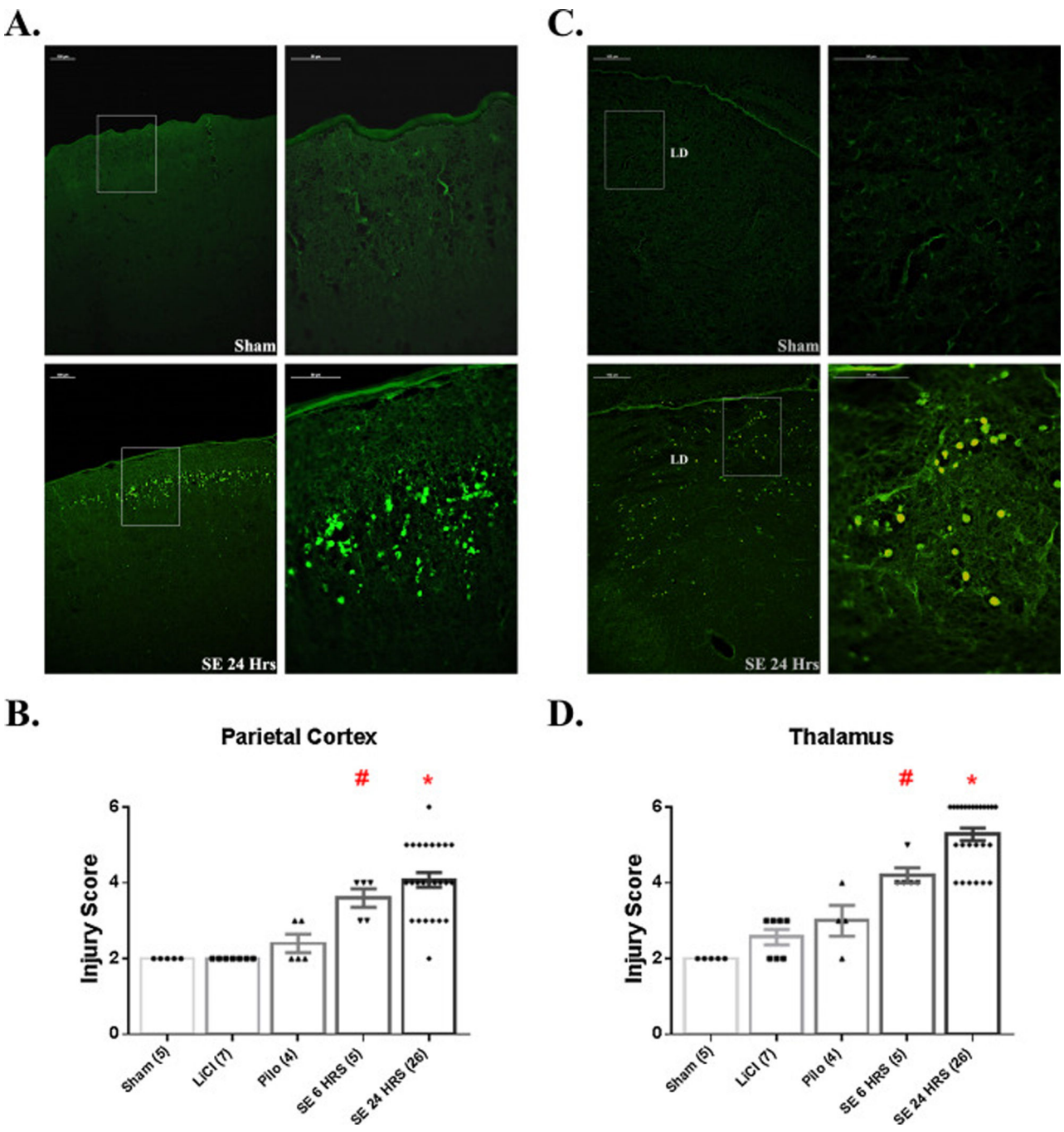

Figure 4.

SE induces neuronal damage in neocortex and thalamus. (A) Images of FJB staining in parietal cortex of Sham and SE24Hrs P7 pups. The image on the right of each row is a higher magnification of the boxed area on the image on the left. As shown, SE induces significant neuronal injury predominantly in layer 2 of the cortex. (B) Graph depicting extent of neuronal injury in parietal cortex, based on a 6-point scoring system. # $p<0.05$: SE 6 HRS vs. Sham, LiCl, Pilo (analyzed by Mann-Whitney). * $p<0.05$: SE 24 HRS vs. Sham, LiCl, Pilo (Mann-Whitney test). (C) Images of FJB staining in thalamus (lateral dorsal

nucleus) of Sham and SE24Hrs P7 pups. The image on the right of each row is a higher magnification of the boxed area on the image on the left. SE results significant neuronal injury at 6 and 24 h post-SE. # $p<0.05$: SE 6 HRS vs. Sham, LiCl, Pilo (Mann-Whitney test). * $p<0.05$: SE 24 HRS vs. Sham, LiCl, Pilo, SE 6 HRS (Mann-Whitney test). Abbreviations: LD=lateral dorsal thalamic nucleus. Scale bars: (A, C) left column=100 μm (low magnification images) and right column 20 μm (high magnification images).

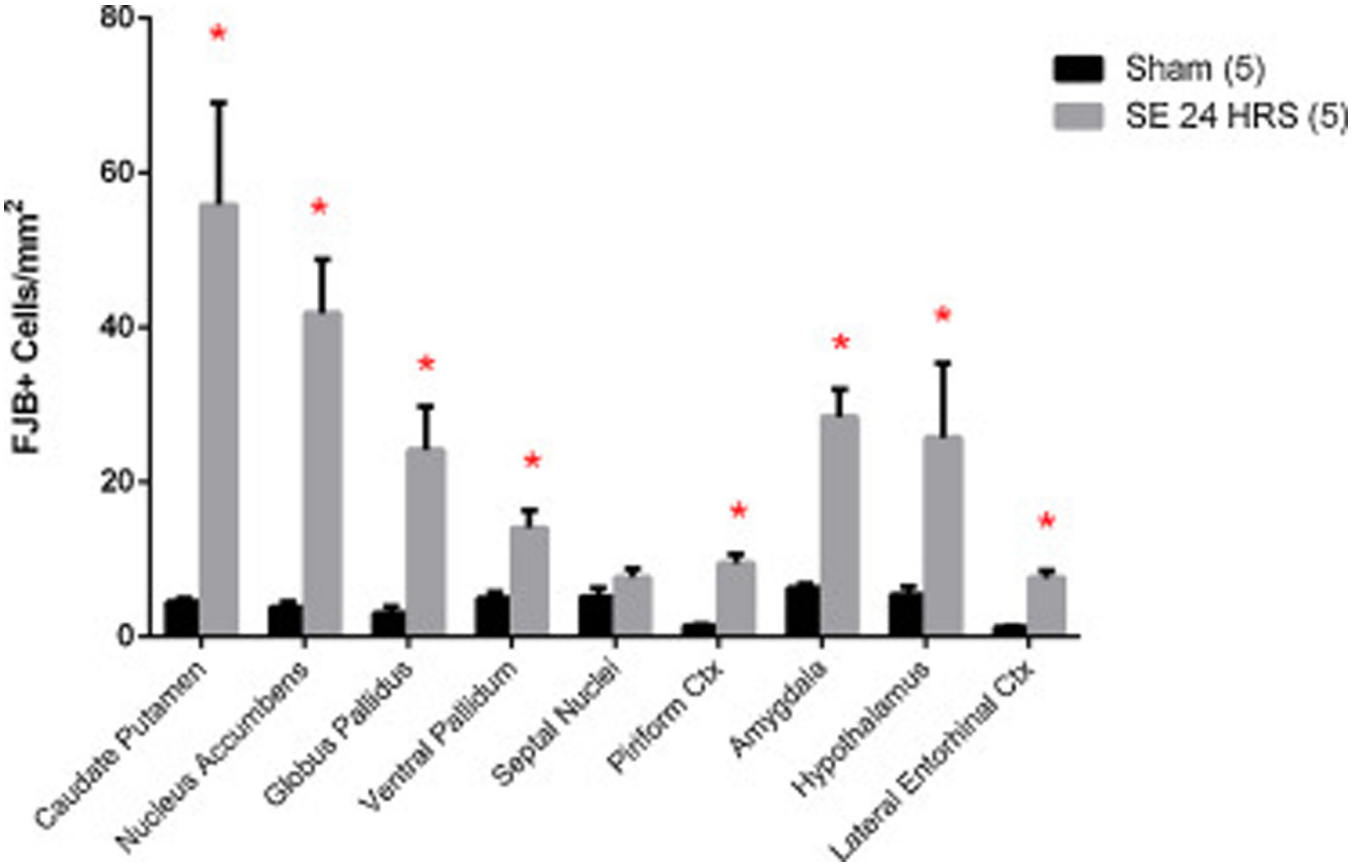

Figure 5.

SE results in neuronal injury in other brain areas. Graph shows other brain regions that were analyzed for neuronal injury among a subset of Sham and SE24Hrs P7 pups. * $p<0.05$: SE 24 HRS vs. Sham (analyzed by Mann-Whitney test). Abbreviations: ctx=cortex.

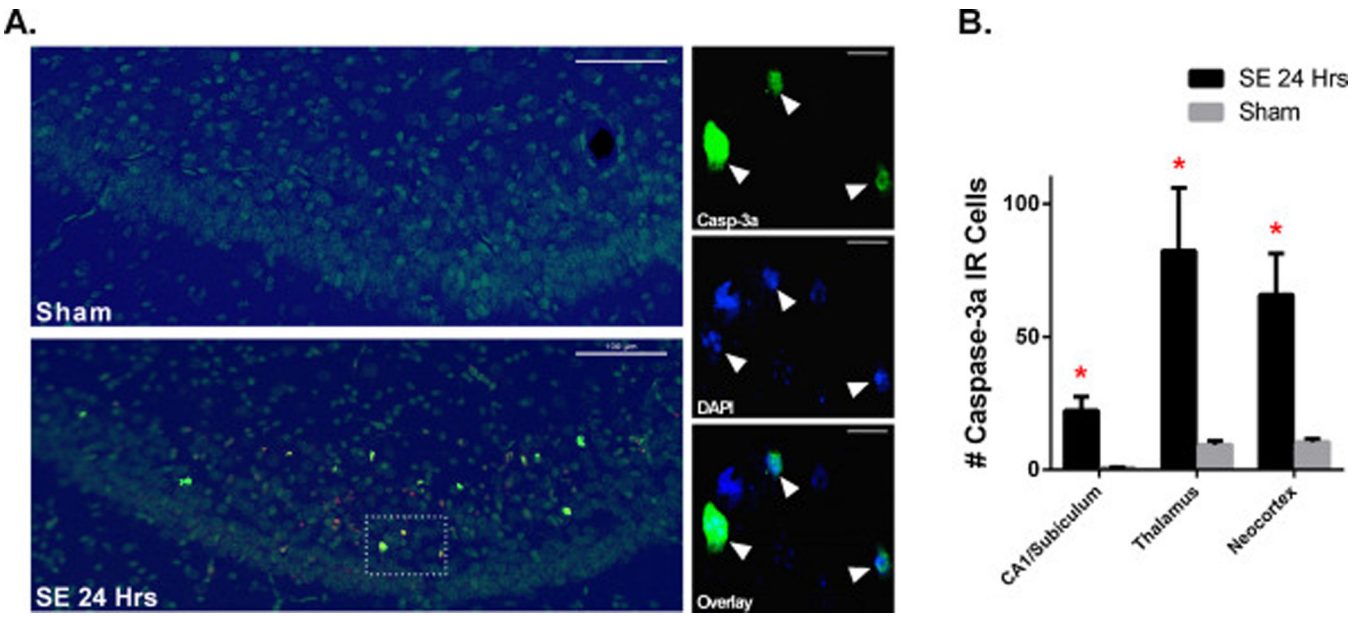

Figure 6.

SE significantly increases caspase-3 activation. (A) Images of overlay of caspase-3a IR (yellow) and DAPI (blue) staining in subiculum of Sham (n=5) and SE24HRS (n=5) pups. On left, overlay of subiculum at low magnification shows distribution of caspase-3a IR cells in subiculum; on right, high magnification images show that caspase-3a IR cells have fragmented nuclei indicative of neuronal cell death in SE24HRS. (B) Graph showing that SE significantly increases caspase-3a IR cells in CA1/Subiculum, thalamus, and neocortex compared to Sham. * $p<0.05$: SE 24 HRS vs. Sham (analyzed by Holm-Sidak test). Scale bars: (A) left column=100 μm (low magnification images) and right column 20 μm (high magnification images).

Table 1

Distribution of neuronal injury varies among brain regions within SE24HRS animals.

	Dorsal					**Ventral**		
	CA1	**CA3**	**DG**	**Parietal Cortex**	**Thalamus**	**CA1**	**CA3**	**DG**
Animal								
1	**17.3**	2.0	0.5	3	**6**	**7.7**	**1.8**	0.6
2	**47.5**	1.1	0.5	**5**	4	**6.2**	**4.4**	**1.2**
3	**61.4**	2.2	0.3	3	4	**6.1**	**2.3**	**0.9**
4	**31.7**	**2.8**	**0.9**	**4**	4	5.9	**1.9**	0.5
5	**13.8**	2.1	0.1	3	4	**7.5**	1.2	0.7
6	3.6	1.0	0.2	3	**6**	2.7	1.4	0.4
7	2.2	**2.2**	0.5	3	**6**	5.6	1.0	0.8
8	3.3	**3.4**	0.3	**5**	**6**	4.7	1.1	0.1
9	1.0	1.5	**0.6**	**4**	**6**	1.0	1.1	0.5
10	1.0	0.6	0.5	**4**	**6**	2.7	1.2	0.3
11	0.9	1.4	0.2	**4**	4	3.1	1.4	0.4
12	4.3	**5.0**	**1.3**	**5**	**6**	5.5	**5.2**	0.7
13	**13.4**	**6.8**	**2.1**	**5**	5	5.5	**1.7**	0.6
14	3.4	**3.6**	**1.5**	**6**	**6**	0.9	0.8	**1.4**
15	1.4	**5.2**	0.2	**5**	**6**	**6.8**	**2.0**	**0.9**
16	9.4	**3.1**	0.2	**4**	**6**	2.1	1.3	0.4
17	4.3	0.9	0.1	**4**	5	1.9	1.0	**1.2**
18	2.0	0.5	0.5	2	**6**	**7.6**	1.2	**1.4**
19	**40.0**	1.4	**1.5**	3	5	**62.2**	**2.0**	**1.6**
20	**12.5**	**3.8**	**2.7**	**4**	**6**	**40.2**	**4.4**	**3.6**
21	**42.5**	0.8	**38.7**	**5**	5	2.0	0.5	**25.2**
22	**17.8**	**2.3**	**1.1**	**5**	5	**6.5**	**1.6**	**1.0**
23	**15.1**	**2.5**	**9.0**	**4**	4	**31.9**	0.8	**7.3**
24	**25.7**	**2.7**	**14.6**	**5**	**6**	**11.6**	**2.9**	**6.0**

	Dorsal					Ventral		
	CA1	**CA3**	**DG**	**Parietal Cortex**	**Thalamus**	**CA1**	**CA3**	**DG**
25	12.0	0.8	**0.9**	**5**	5	**7.4**	**2.8**	**1.3**
26	**28.4**	**4.6**	**1.7**	**4**	5	**10.1**	**3.8**	**2.7**
Average:	**16.0**	**2.5**	**3.1**	**4.1**	**5.3**	**9.8**	**1.9**	**2.4**
Median:	**12.3**	**2.2**	**0.6**	**4.0**	**5.5**	**6.0**	**1.5**	**0.9**

Table showing distribution of neuronal injury in individual pups. Neuronal injury values in *bold* are above the median. CA1, CA3, and DG values represent FJB+ cells/mm while parietal cortex and thalamus values represent an injury severity score 1–6 (see methods 2.4).